REHABILITATION OF THE LOWEST-ORDER RAVIART-THOMAS ELEMENT ON QUADRILATERAL GRIDS*

PAVEL B. BOCHEV† AND DENIS RIDZAL‡

Abstract. A recent study [4] reveals that convergence of finite element methods using $H(\mathrm{div}\,,\Omega)$-compatible finite element spaces deteriorates on non-affine quadrilateral grids. This phenomena is particularly troublesome for the lowest-order Raviart-Thomas elements, because it implies loss of convergence in some norms for finite element solutions of mixed and least-squares methods. In this paper we propose reformulation of finite element methods, based on the natural mimetic divergence operator [22], which restores the order of convergence.

Reformulations of mixed Galerkin and least-squares methods for the Darcy equation illustrate our approach. We prove that reformulated methods converge optimally with respect to a norm involving the mimetic divergence operator. Furthermore, we prove that standard and reformulated versions of the mixed Galerkin method lead to *identical* linear systems, but the two versions of the least-squares method are veritably different. The surprising conclusion is that the degradation of convergence in the mixed method on non-affine quadrilateral grids is superficial, and that the lowest order Raviart-Thomas elements are safe to use in this method. However, the breakdown in the least-squares method is real, and there one should use our proposed reformulation.

AMS subject classifications. 65F10, 65F30, 78A30

1. Introduction. We consider finite element solution of the elliptic boundary value problem

$$\left\{\begin{array}{rl} \nabla\cdot\mathbf{u}+\sigma\Theta_0 p &= f \\ \nabla p+\Theta_1^{-1}\mathbf{u} &= 0 \end{array}\right. \quad \text{in } \Omega \quad \text{and} \quad \begin{array}{rl} p &= 0 \ \text{ on } \Gamma_D \\ \boldsymbol{n}\cdot\mathbf{u} &= 0 \ \text{ on } \Gamma_N, \end{array} \tag{1.1}$$

where $\Omega\subset\Re^2$ has Lipschitz-continuous boundary $\partial\Omega=\Gamma_D\cup\Gamma_N$, $\boldsymbol{n}$ is the unit outward normal to $\partial\Omega$, Θ_1 is a symmetric tensor, Θ_0 is a real valued function, and σ is a non-dimensional parameter that is either 0 or 1. Regarding Θ_1 and Θ_0 we will assume that there exists a constant $\alpha>0$ such that for every $\boldsymbol{x}\in\Omega$ and $\boldsymbol{\xi}\in\Re^2$

$$\frac{1}{\alpha}\boldsymbol{\xi}^T\boldsymbol{\xi}\le\boldsymbol{\xi}^T\Theta_1(\boldsymbol{x})\boldsymbol{\xi}\le\alpha\boldsymbol{\xi}^T\boldsymbol{\xi} \ \text{ and } \ \frac{1}{\alpha}\le\Theta_0(\boldsymbol{x})\le\alpha\,. \tag{1.2}$$

Equations (1.1) are often called the Darcy problem and provide a simplified model of a single phase flow in porous media. In this context, p is the pressure, $\mathbf{u}$ is the Darcy velocity and Θ_1 is the permeability tensor divided by the viscosity. The use of this first-order system as a basis for a finite element method stems from the fact that in porous media flow the vector variable $\mathbf{u}$ is more important than the pressure p. In such cases numerical methods that compute accurate, locally conservative velocity approximations are favored.

*Received by the editors Month ??, 2007; accepted for publication (in revised form) Month ??, 2007; published electronically Month ??, 2007. Sandia is a multiprogram laboratory operated by Sandia Corporation, a Lockheed Martin Company, for the United States Department of Energy under contract DE-AC04-94-AL85000.
http://www.siam.org/journals/sinum/????.html.

†Sandia National Laboratories, Applied Mathematics and Applications, P.O. Box 5800, MS 1320, Albuquerque, NM 87185-1320 (pbboche@sandia.gov).

‡Sandia National Laboratories, Optimization and Uncertainty Quantification, P.O. Box 5800, MS 1320, Albuquerque, NM 87185-1320 (dridzal@sandia.gov).

Two such methods are the mixed Galerkin method [12] and the locally conservative least-squares method [7, 8, 14]. The main focus of this paper will be on implementations of these two methods with the lowest-order quadrilateral Raviart-Thomas elements (RT_0) [21, 12]. Several reasons motivate our interest in these elements. Quadrilateral grids are widely used in the petroleum industry for porous media flow simulations and there are connections between conservative finite difference methods for (1.1) and mixed methods implemented with the lowest order $H(\mathrm{div}\,,\Omega)$-compatible spaces; see [1, 5, 24] and the references therein. Our study is also prompted by the recent work of Arnold et al. [4]. This paper asserts that the accuracy of $H(\mathrm{div}\,,\Omega)$-conforming finite element spaces deteriorates on non-affine quadrilateral grids, which in turn leads to reduced orders of convergence in finite element methods. Arnold et al. [4] support this assertion by examples that show reduced convergence in $H(\mathrm{div}\,,\Omega)$ of the vector variable in the mixed method, and examples which suggest that in the least-squares method loss of accuracy also spreads to pressure approximations.

These examples are particularly damning for low-order elements because for them the degradation of accuracy in the methods takes the form of a total loss of convergence in some norms for one or both variables. The main goal of this paper is to restore confidence in RT_0 elements and show that with some simple modifications in the finite element methods they can be safely used on general, shape regular, but not necessarily affine quadrilateral grids.

The proposed reformulation of the mixed and least-squares methods is motivated by mimetic finite difference methods [22]. A mimetic discretization of (1.1) uses the so-called *natural mimetic* divergence, DIV and *derived* gradient, $\overline{\mathsf{GRAD}}$ operators; see [16, 17]. Of particular interest to us is DIV which is constructed using the coordinate-invariant definition [2, p.188]

$$\nabla\cdot\mathbf{u}(\boldsymbol{x}) = \lim_{\kappa\ni\boldsymbol{x};\,\mu(\kappa)\to 0} \frac{\displaystyle\int_{\partial\kappa}\mathbf{u}\cdot\boldsymbol{n}\,dS}{\mu(\kappa)} \tag{1.3}$$

of the divergence operator[1]. The result is a discrete operator[2] that maps face-based values (the fluxes of $\mathbf{u}$) onto cell-based constants. Because DIV acts on the same set of degrees of freedom as used to define the lowest-order Raviart-Thomas space, its action can be extended to that space in a natural way. This is the key to our *mimetic* reformulation of finite element methods, in which the main idea is to replace[3] the analytic divergence $\nabla\cdot$ by the natural divergence DIV.

A somewhat unexpected byproduct of our analysis is a theorem which shows that the mimetic reformulation of the mixed method is actually equivalent to its standard version, in the sense that the two methods generate identical linear algebraic systems with identical solutions. Since in the mimetic reformulation $\mathsf{DIV}(\mathbf{u}^h)$ converges to

[1] In this definition κ is a bounded region and $\mu(\kappa)$ denotes its measure. The mimetic approximation of $\nabla\cdot\mathbf{u}$ on an element κ, belonging to a finite element partition $\mathcal{T}_h$ of Ω, is defined by the right hand side in this formula, assuming that $\mathbf{u}$ and $\boldsymbol{n}$ are constant on the faces of κ.

[2] For brevity we call this operator "natural divergence".

[3] A perfectly valid alternative solution is to divide each element into two affine triangles and simply use an RT_0 space on triangles [19]. Nonetheless, quadrilateral elements may still be favored for the following reasons. When a quadrilateral grid is transformed into a triangular one by the above procedure, the number of faces increases by a number equal to the number of elements in the original mesh. Because in the RT_0 space each face is associated with a degree of freedom, this means that the size of the discretized problem will also increase by the same number without formally increasing its accuracy. Second for problems with advection, quadrilateral grids are easier to align with the flow which reduces the amount of artificial numerical diffusion.

the divergence of the exact solution, it follows that the same must be true for the solution of the standard mixed method. In other words, the flux degrees of freedom in the mixed Galerkin solution do contain accurate information about the divergence of the exact solution. The reason $\nabla\cdot$ fails to recover this information on non-affine quads is that it acts on the flux data *indirectly* via basis functions defined by the Piola transform, which makes the result dependent upon the element shape[4]. In contrast, DIV is able to always recover accurate divergence approximation because it acts *directly* on the flux degrees of freedom, which makes its action independent of the element shape. It follows that the loss of convergence in the mixed method is superficial, and that this method can be safely used on non-affine quadrilateral grids.

Unlike the mixed method, mimetic reformulation of the least-squares method turns out to be veritably different from its standard finite element realization and the loss of convergence in this method, reported in [4], is genuine. We refine the conclusions of [4] by showing that for Darcy problems that include a "reaction" term ($\sigma = 1$) the loss of accuracy does not spread to the pressure approximation. However, the "information content" of the velocity approximation is ruined and using DIV in lieu of $\nabla\cdot$ to extract divergence information does not help much. Thus, the breakdown in the least-squares method is real and for general quadrilateral grids one should use our proposed reformulation.

The paper is organized as follows. Section 2 reviews notation and definitions of finite element spaces. Section 3 discusses the natural divergence operator, its properties, and extension to the lowest-order Raviart-Thomas elements. Section 4 presents mimetic reformulations of mixed and least-squares methods. Section 5 contains analyses of these methods. Numerical results are collected in Section 6.

2. Notation and quotation of results. For $p > 0$, $H^p(\Omega)$ denotes the Sobolev space of order p with norm and inner product denoted by $\|\cdot\|_p$ and $(\cdot,\cdot)_p$, respectively. When $p = 0$, we use the standard notation $L^2(\Omega)$. The symbol $|\cdot|_k$, $0 \le k \le p$, denotes the kth seminorm on $H^p(\Omega)$, while $H^1_D(\Omega)$ is the subspace of $H^1(\Omega)$ consisting of all functions that vanish on Γ_D. The sets $H(\mathrm{div}\,,\Omega) = \{\mathbf{u} \in (L^2(\Omega))^2 \;\mid\; \nabla\cdot\mathbf{u} \in L^2(\Omega)\}$, and its subset $H_N(\mathrm{div}\,,\Omega) = \{\mathbf{v} \in H(\mathrm{div}\,,\Omega) \;\mid\; \mathbf{v}\cdot\boldsymbol{n} = 0 \quad \text{on } \Gamma_N\}$ are Hilbert spaces when equipped with the graph norm $\|\mathbf{u}\|_{\mathrm{div}} = (\|\mathbf{u}\|_0^2 + \|\nabla\cdot\mathbf{u}\|_0^2)^{1/2}$.

Throughout the paper $\mathcal{T}_h$ is partition of Ω into convex quadrilateral elements κ, $\mathcal{N}_h$ is the set of nodes $\boldsymbol{x}_i$ in $\mathcal{T}_h$ and $\mathcal{F}_h$ is the set of oriented faces $\boldsymbol{f}_i$ in $\mathcal{T}_h$. A face is oriented by choosing a unit normal $\boldsymbol{n}_{\boldsymbol{f}}$ and an element is oriented by choosing a unit normal $\boldsymbol{n}_\kappa$ to its boundary $\partial\kappa$. By default, all elements are oriented as sources so that $\boldsymbol{n}_\kappa$ is the outer unit normal to $\partial\kappa$.

We assume that the elements in $\mathcal{T}_h$ satisfy the usual conditions required of finite element partitions; see [13, pp.38–51]. In what follows we restrict attention to shape-regular partitions $\mathcal{T}_h$ where each κ is a bilinear image of the reference square $\hat\kappa = [-1,1]^2$. We recall that for such partitions there exists a positive α such that

$$\frac{1}{\alpha}\mu(\kappa) \le \|\det D\Phi_\kappa\|_{\infty,\hat\kappa} \le \alpha\mu(\kappa) \quad \forall\kappa \in \mathcal{T}_h\,; \tag{2.1}$$

see [15, p.105]. In (2.1) $D\Phi_\kappa(\hat{\boldsymbol{x}})$ is the derivative of the bilinear function $\Phi_\kappa(\hat{\boldsymbol{x}})$ that maps $\hat\kappa$ to a given quadrilateral κ. When the range of Φ_κ is clear from the context we will skip the subscript κ. There also holds (see [15, p.105])

$$\det D\Phi_\kappa(\hat{\boldsymbol{x}}) > 0 \;\; \forall\hat{\boldsymbol{x}} \in \hat\kappa \quad \text{and} \quad \mu(\kappa) = \det D\Phi_\kappa(0,0)\mu(\hat\kappa)\,. \tag{2.2}$$

[4]This is also the reason why formal finite element analysis fails to recognize that the mixed Galerkin solution does contain accurate divergence information.

The first property follows from the convexity of each κ.

$P_{qr}(V)$ denotes polynomial functions on a region $V \subset \Re^2$, whose degree in x and y does not exceed q and r, respectively. Thus, $P_{00}(V)$ is the set of constant polynomials on V; P_{11} is the set of bilinear polynomials on V and so on.

Since our focus is on low-order methods, for the mixed Galerkin method we consider pressure approximations by the piecewise constant space

$$Q_0 = \{p^h \in L^2(\Omega) \,|\, p^h|_\kappa \in P_{00}(\kappa) \;\; \forall \kappa \in \mathcal{T}_h\}\,, \tag{2.3}$$

and velocity approximations by the lowest-order Raviart-Thomas space

$$RT_0 = \{\mathbf{u}^h \in H(\mathrm{div}\,,\Omega) \,|\, \mathbf{u}^h|_\kappa = \mathcal{P}_\kappa \circ \hat{\mathbf{u}}^h;\;\; \hat{\mathbf{u}}^h \in P_{10}(\hat{\kappa}) \times P_{01}(\hat{\kappa}) \;\; \forall \kappa \in \mathcal{T}_h\}, \tag{2.4}$$

where $\mathcal{P}_\kappa = \det(D\Phi(\hat{\boldsymbol{x}}))^{-1} D\Phi(\hat{\boldsymbol{x}})$ is the Piola transform; see [12, p.97]. The least-squares method uses the same space for the velocity, and the C^0 Lagrangian space

$$Q_1 = \{p^h \in C^0(\overline{\Omega}); p^h|_\kappa = \hat{p} \circ \Phi_\kappa^{-1};\;\; \hat{p} \in P_{11}(\hat{\kappa}) \;\; \forall \kappa \in \mathcal{T}_h\} \tag{2.5}$$

for the pressure approximation.

Finite element spaces are restricted by boundary conditions. RT_0^N is the subspace of RT_0 such that $\mathbf{u}^h \cdot \boldsymbol{n} = 0$ on Γ_N, and Q_1^D is the subspace of Q_1 such that $p^h = 0$ on Γ_D. No boundary conditions are imposed on Q_0.

REMARK 1. *The mapping Φ_κ is affine if and only if κ is a parallelogram. Therefore, in general, RT_0 and Q_1 are not piecewise polynomial spaces.*

The unisolvent set of Q_0 consists of the element averages

$$\Lambda(Q_0) = \{l_\kappa \,|\, l_\kappa(p) = \int_\kappa p dx;\;\; \kappa \in \mathcal{T}_h\}\,, \tag{2.6}$$

the unisolvent set of Q_1 is given by the nodal values

$$\Lambda(Q_1) = \{l_{\boldsymbol{x}} \,|\, l_{\boldsymbol{x}}(p) = \int_\Omega \delta(\boldsymbol{x}) p dx;\;\; \boldsymbol{x} \in \mathcal{N}_h\}\,, \tag{2.7}$$

and the unisolvent set for RT_0 is the average flux across element faces

$$\Lambda(RT_0) = \{l_{\boldsymbol{f}} \,|\, l_{\boldsymbol{f}}(\mathbf{v}) = \int_{\boldsymbol{f}} \mathbf{v} \cdot \boldsymbol{n}\, dS;\;\; \boldsymbol{f} \in \mathcal{F}_h\}\,. \tag{2.8}$$

The symbols $\{p_\kappa\}$, $\{p_{\boldsymbol{x}}\}$, and $\{\mathbf{u}_{\boldsymbol{f}}\}$ stand for the basis sets of Q_0, Q_1 and RT_0, which are dual to (2.6), (2.7) and (2.8), respectively; see [13, 12] for further details.

$\mathcal{I}_{Q_0}$, $\mathcal{I}_{Q_1}$, and $\mathcal{I}_{RT_0}$ are the interpolation operators into Q_0, Q_1, and RT_0, induced by the degrees of freedom in (2.6)-(2.8). Domains of $\mathcal{I}_{Q_1}$ and $\mathcal{I}_{RT_0}$ consist of those functions in $H^1(\Omega)$ and $H(\mathrm{div}\,,\Omega)$ for which the functionals in (2.7) and (2.8) are meaningful. For the domain of $\mathcal{I}_{RT_0}$ we will use the space

$$W(\Omega) = \{\mathbf{u} \in (L^s(\Omega))^2 \,|\, \nabla \cdot \mathbf{u} \in L^2(\Omega);\;\; s > 2\}\,. \tag{2.9}$$

With this choice $\mathcal{I}_{RT_0}$ is uniformly bounded as an operator $W \mapsto RT_0$; see [12, p.125]:

$$\|\mathcal{I}\mathbf{u}\|_{\mathrm{div}} \le C \|\mathbf{u}\|_W\,. \tag{2.10}$$

When the range of the interpolation operator is clear from the type of its argument we skip the space designation and simply write $\mathcal{I}$.

Approximation properties of interpolation operators are as follows. The L^2 projection $\mathcal{I}_{Q_0}$ is first-order accurate (see [15, p.108]):

$$\|p - \mathcal{I}_{Q_0} p\|_0 \le Ch\|p\|_1 \quad \forall p \in H^1(\Omega)\,. \tag{2.11}$$

On shape-regular quadrilateral grids $\mathcal{I}_{RT_0}$ is first-order[5] accurate in L^2:

$$\|\mathbf{u} - \mathcal{I}_{RT_0}\mathbf{u}\|_0 \le Ch\|\mathbf{u}\|_1 \quad \forall \mathbf{u} \in H^1(\Omega)^2\,; \tag{2.12}$$

see [4, Theorem 4.1]. The nodal interpolant $\mathcal{I}_{Q_1}$ satisfies the error bound

$$\|p - \mathcal{I}_{Q_1} p\|_0 + h\|\nabla(p - \mathcal{I}_{Q_1} p)\|_0 \le Ch\|p\|_2 \quad \forall p \in H^2(\Omega)\,; \tag{2.13}$$

see [15, p.107] and [3]. Next lemma states an important property of the divergence operator that will be needed later.

LEMMA 2.1. *Divergence is a surjective mapping $H_N(\mathrm{div}\,,\Omega) \cap W(\Omega) \mapsto L^2(\Omega)$ with a continuous lifting from $L^2(\Omega)$ into $H_N(\mathrm{div}\,,\Omega) \cap W(\Omega)$, that is, for every $q \in L^2(\Omega)$ there exists $\mathbf{u}_q \in H_N(\mathrm{div}\,,\Omega) \cap W(\Omega)$ such that*

$$q = \nabla \cdot \mathbf{u}_q \quad \textit{and} \quad \|\mathbf{u}_q\|_W \le C\|q\|_0\,. \tag{2.14}$$

For details we refer to [12, p.136].

3. Extension of DIV to RT_0. Definition of the natural divergence DIV is based on the coordinate-independent characterization of $\nabla \cdot \mathbf{u}$ in (1.3), applied to each cell $\kappa \in \mathcal{T}_h$. Let $\mathcal{F}_h^*$ and $\mathcal{T}_h^*$ denote the duals of $\mathcal{F}_h$ and $\mathcal{T}_h$, i.e., collections of real numbers $\{F_{\boldsymbol{f}}\}$, $\{K_\kappa\}$ associated with the oriented faces and cells in the mesh. Clearly, $\mathcal{F}_h^*$ and $\mathcal{T}_h^*$ are isomorphic[6] to RT_0 and Q_0, respectively, and so, we denote their elements by the same symbols.

The natural divergence is a mapping $\mathsf{DIV} : \mathcal{F}_h^* \mapsto \mathcal{T}_h^*$ defined by

$$\mathsf{DIV}(\mathbf{u}^h)|_\kappa = \frac{1}{\mu(\kappa)} \sum_{\boldsymbol{f} \in \mathcal{F}_h(\kappa)} \sigma_{\boldsymbol{f}} F_{\boldsymbol{f}}\,; \qquad \forall \kappa \in \mathcal{T}_h\,, \tag{3.1}$$

where $\mathbf{u}^h \in \mathcal{F}_h^*$, $\mathcal{F}_h(\kappa)$ is the set of oriented faces of κ and

$$\sigma_{\boldsymbol{f}} = \begin{cases} 1 & \text{if } \boldsymbol{n}_{\boldsymbol{f}} = \boldsymbol{n}_\kappa \\ -1 & \text{if } \boldsymbol{n}_{\boldsymbol{f}} = -\boldsymbol{n}_\kappa \end{cases}$$

Note that $F_{\boldsymbol{f}}$ are also the degrees of freedom that define vector fields in RT_0:

$$\mathbf{u}^h = \sum_{\boldsymbol{f} \in \mathcal{F}_h} F_{\boldsymbol{f}} \mathbf{u}_{\boldsymbol{f}} \quad \forall \mathbf{u}^h \in RT_0\,.$$

Therefore, the action of DIV can be extended to RT_0 vector fields by simply adopting formula (3.1) to compute the discrete divergence of $\mathbf{u}^h \in RT_0$. This defines an

[5] On non-affine grids the divergence error of Raviart-Thomas spaces drops by one order. As a result, $\nabla \cdot \mathcal{I}_{RT_0}(\mathbf{u})$ does not converge to $\nabla \cdot \mathbf{u}$; see [4, Theorem 4.2]. However, as we shall see, the natural divergence of the interpolant is first-order accurate.

[6] This is the key reason why many conservative finite difference methods for (1.1) can be related to low-order implementations of the mixed method – both types of schemes share the same set of degrees of freedom.

operator $\mathsf{DIV} : RT_0 \mapsto Q_0$ which we will use to reformulate mixed and least-squares methods. It is easy to see that for the basis $\{\mathbf{u}_{\boldsymbol{f}}\}$ of RT_0,

$$\mathsf{DIV}(\mathbf{u}_{\boldsymbol{f}}) = \frac{\sigma_{\boldsymbol{f}}}{\mu(\kappa)}; \quad \forall \boldsymbol{f} \in \mathcal{F}_h\,. \tag{3.2}$$

The next lemma states an important property of the natural divergence.

LEMMA 3.1. *The natural divergence* DIV *has a pointwise Commuting Diagram Property (CDP)*

$$\begin{array}{ccccc} & & W(\Omega) & \stackrel{\nabla\cdot}{\longrightarrow} & L^2(\Omega) & \\ \mathcal{I}_{RT_0} & & \downarrow & & \downarrow & \mathcal{I}_{Q_0} \\ & & RT_0 & \stackrel{\mathsf{DIV}}{\longrightarrow} & Q_0 & \end{array} \tag{3.3}$$

Proof. We need to prove that $\mathsf{DIV}\,(\mathcal{I}_{RT_0}\mathbf{u}) = \mathcal{I}_{Q_0}(\nabla\cdot\mathbf{u})$ for all $\mathbf{u} \in W(\Omega)$. From definition (3.1) and equation (3.2) it follows that

$$\mathsf{DIV}\,(\mathcal{I}_{RT_0}\mathbf{u})\,|_\kappa = \mathsf{DIV} \sum_{\boldsymbol{f}\in\mathcal{F}_h(\kappa)} F_{\boldsymbol{f}}\mathbf{u}_{\boldsymbol{f}} = \frac{1}{\mu(\kappa)} \sum_{\boldsymbol{f}\in\mathcal{F}_h(\kappa)} \sigma_{\boldsymbol{f}} F_{\boldsymbol{f}}\,.$$

On the other hand, from (2.6) and the Divergence Theorem

$$\mathcal{I}_{Q_0}\,(\nabla\cdot\mathbf{u})\,|_\kappa = \frac{1}{\mu(\kappa)}\int_\kappa \nabla\cdot\mathbf{u}\,dx = \frac{1}{\mu(\kappa)}\int_{\partial\kappa} \mathbf{u}\cdot\boldsymbol{n}\,dS = \frac{1}{\mu(\kappa)} \sum_{\boldsymbol{f}\in\mathcal{F}_h(\kappa)} \int_{\boldsymbol{f}} \mathbf{u}\cdot\boldsymbol{n}\,dS\,.$$

CDP follows from the identity

$$\int_{\boldsymbol{f}} \mathbf{u}\cdot\boldsymbol{n}\,dS = \sigma_{\boldsymbol{f}} F_{\boldsymbol{f}}\,.$$

□

A discrete version of Lemma 2.1 holds for the natural divergence.

LEMMA 3.2. *The natural divergence is a surjective mapping* $RT_0 \mapsto Q_0$ *with a continuous lifting from* Q_0 *into* RT_0*, that is, for every* $q^h \in Q_0$ *there exists* $\mathbf{u}_q^h \in RT_0$ *such that*

$$q^h = \mathsf{DIV}(\mathbf{u}_q^h) \quad \textit{and} \quad \|\mathbf{u}_q^h\|_0 + \|\mathsf{DIV}(\mathbf{u}_q^h)\|_0 \le C\|q^h\|_0\,. \tag{3.4}$$

Proof. To show that DIV is surjective we use CDP and the fact that analytic divergence is a surjective mapping $W(\Omega) \mapsto L^2(\Omega)$ (Lemma 2.1). Any $q^h \in Q_0$ is also in $L^2(\Omega)$ and so, there exists $\mathbf{u}_q \in H_N(\mathrm{div}\,,\Omega) \cap W(\Omega)$ such that $\nabla\cdot\mathbf{u}_q = q^h$. Let $\mathbf{u}_q^h = \mathcal{I}_{RT_0}(\mathbf{u}_q)$. From CDP it follows that $\mathsf{DIV}(\mathbf{u}_q^h) = \mathcal{I}_{Q_0}(\nabla\cdot\mathbf{u}_q) = \mathcal{I}_{Q_0}(q^h) = q^h$.

Because by construction $\mathsf{DIV}(\mathbf{u}_q^h) = q^h$, to prove that the lifting of DIV from Q_0 into RT_0 is continuous it suffices to show that $\|\mathbf{u}_q^h\|_0 = \|\mathcal{I}_{RT_0}(\mathbf{u}_q)\|_0 \le \|q^h\|_0$. Using (2.10) (uniform boundedness of $\mathcal{I}_{RT_0}$) and (2.14) in Lemma 2.1 we see that

$$\|\mathcal{I}_{RT_0}(\mathbf{u}_q)\|_0 \le \|\mathcal{I}_{RT_0}(\mathbf{u}_q)\|_{\mathrm{div}} \le C\|\mathbf{u}_q\|_W \le C\|q^h\|_0\,.$$

This proves the lemma. □

REMARK 2. *According to Lemma 2.1* $\nabla\cdot$ *is surjection* $H_N(\mathrm{div}\,,\Omega) \mapsto L^2(\Omega)$. *In the mixed method the domain and the range of this operator are approximated by* RT_0 *and* Q_0 *elements, respectively. However, on non-affine quadrilateral grids* $\nabla\cdot RT_0 \neq Q_0$, *and the surjective property connecting the domain and the range of* $\nabla\cdot$ *is lost.*[7] *By replacing the analytic divergence by* DIV *surjectivity is restored. As a result, if* RT_0 *is to approximate the domain of the divergence and* Q_0 *- its range, then the approximation of* $\nabla\cdot$, *which is compatible with its surjective property, is given by* DIV *rather than* $\nabla\cdot$. *In other words,* DIV *provides a better approximation of* $\nabla\cdot$ *on* RT_0 *than the usual finite element practice of restricting the analytic operator to the finite element space. This fact validates the mimetic reformulation strategy presented in the next two sections.*

REMARK 3. *The surjective property of* DIV, *and its lack thereof in* $\nabla\cdot$, *is a direct consequence of the way these operators act on the flux degrees of freedom. As we have already noted in Section 1,* DIV *operates directly on these degrees of freedom, whereas the action of* $\nabla\cdot$ *is indirect via basis functions defined by the Piola transform. As a result, the divergence approximation computed by* DIV *depends only on the flux data and not on the element shape.*

The following two lemmata will prove useful later.

LEMMA 3.3. *For every* $\mathbf{u}^h \in RT_0$ *there holds*

$$\int_\kappa \nabla\cdot\mathbf{u}^h\,dx = \int_\kappa \mathsf{DIV}(\mathbf{u}^h)\,dx\,; \quad \kappa\in\mathcal{T}_h\,. \tag{3.5}$$

Proof. It is enough to show (3.5) for a basis function $\mathbf{u}_{\boldsymbol{f}}$ associated with a face $\boldsymbol{f}\in\partial\kappa$. Using (3.2) and definition of the basis functions,

$$\int_\kappa \mathsf{DIV}(\mathbf{u}_{\boldsymbol{f}})\,dx = \frac{\sigma_{\boldsymbol{f}}}{\mu(\kappa)}\int_\kappa dx = \sigma_{\boldsymbol{f}} = \int_{\partial\kappa}\boldsymbol{n}\cdot\mathbf{u}_{\boldsymbol{f}}\,dS = \int_\kappa \nabla\cdot\mathbf{u}_{\boldsymbol{f}}\,dx\,.$$

□

LEMMA 3.4. *Assume that* $\mathcal{T}_h$ *is shape-regular. There is a positive constant* C_D *such that*

$$\|\nabla\cdot\mathbf{u}^h\|_0 \le C_D\|\mathsf{DIV}(\mathbf{u}^h)\|_0\,. \tag{3.6}$$

Proof. It suffices to show (3.6) for one element κ and one basis function $\mathbf{u}_{\boldsymbol{f}}$ with $\boldsymbol{f}\in\partial\kappa$. After changing variables and noting that the Jacobian is positive (see (2.2))

$$\|\nabla\cdot\mathbf{u}_{\boldsymbol{f}}\|^2_{0,\kappa} = \int_\kappa(\nabla\cdot\mathbf{u}_{\boldsymbol{f}})(\nabla\cdot\mathbf{u}_{\boldsymbol{f}})\,dx = \int_{\hat\kappa}(\nabla_{\hat{\boldsymbol{x}}}\cdot\hat{\mathbf{u}}_{\hat{\boldsymbol{f}}})(\nabla_{\hat{\boldsymbol{x}}}\cdot\hat{\mathbf{u}}_{\hat{\boldsymbol{f}}})(\det D\Phi)^{-1}\,d\hat{x}\,,$$

where $\hat{\boldsymbol{f}}$ is one of the faces of the reference element $\hat\kappa$. From (2.4) and (2.8) it follows that

$$\hat{\mathbf{u}}_{\hat{\boldsymbol{f}}} = \frac{1}{4}\begin{bmatrix}1\pm x\\ 0\end{bmatrix} \quad\text{or}\quad \hat{\mathbf{u}}_{\hat{\boldsymbol{f}}} = \frac{1}{4}\begin{bmatrix}0\\ 1\pm y\end{bmatrix}, \quad\text{and}\quad \nabla_{\hat{\boldsymbol{x}}}\cdot\hat{\mathbf{u}}_{\hat{\boldsymbol{f}}} = 1/4\,.$$

[7] The reason why stability of the mixed method is not ruined on such grids is that the following weak CDP holds for $\nabla\cdot$: $\mathcal{I}_{Q_0}(\nabla\cdot\mathcal{I}_{RT_0}(\mathbf{u})) = \mathcal{I}_{Q_0}(\nabla\cdot\mathbf{u})$, i.e.,

$$\int_\Omega q^h\nabla\cdot\mathbf{u}\,dx = \int_\Omega q^h\nabla\cdot\mathcal{I}_{RT_0}(\mathbf{u})\,dx\,.$$

According to Fortin's Lemma this is enough for the inf-sup condition to hold; see [12, p.138].

Using the Mean Value Theorem, the lower bound in (2.1), (3.2), and $\mu(\hat{\kappa}) = 4$:

$$\|\nabla \cdot \mathbf{u}_{\boldsymbol{f}}\|^2_{0,\kappa} = \frac{1}{16}\int_{\hat{\kappa}} (\det D\Phi)^{-1}\, d\hat{x} = \frac{\mu(\hat{\kappa})}{16 \det D\Phi(\hat{x}^*)} \leq \frac{\alpha\mu(\hat{\kappa})}{16\mu(\kappa)} = \frac{\alpha}{4}\|\mathsf{DIV}(\mathbf{u}_{\boldsymbol{f}})\|^2_{0,\kappa}\,.$$

Thus, (3.6) holds with $C_D = \alpha/4$. □

4. Mimetic reformulation of finite element methods. We begin with a brief summary of the standard mixed method [12] and the locally conservative least-squares method [8]. For further information about related least-squares methods we refer to [6, 14, 7] and the references cited therein.

4.1. Standard methods. The standard mixed finite element method for (1.1) solves the following variational problem: *seek* $\mathbf{u}^h \in RT_0^N$ *and* $p^h \in Q_0$ *such that*

$$\left\{\begin{array}{lll} \displaystyle\int_\Omega \mathbf{u}^h \Theta_1^{-1}\mathbf{v}^h\, dx - \int_\Omega p^h \nabla\cdot\mathbf{v}^h\, dx &= 0 & \forall \mathbf{v}^h \in RT_0^N \\ \displaystyle\int_\Omega \nabla\cdot\mathbf{u}^h q^h\, dx + \sigma\int_\Omega p^h\Theta_0 q^h\, dx &= \displaystyle\int_\Omega f q^h\, dx & \forall q^h \in Q_0 \end{array}\right. . \tag{4.1}$$

The second method in our study is a compatible least-squares method for (1.1). In this method the finite element approximation is determined by seeking the minimizer of the least-squares quadratic functional

$$J(p^h,\mathbf{u}^h;f) = \|\Theta_0^{-1/2}(\nabla\cdot\mathbf{u}^h + \sigma\Theta_0 p^h - f)\|_0^2 + \|\Theta_1^{1/2}(\nabla p^h + \Theta_1^{-1}\mathbf{u}^h)\|_0^2 \tag{4.2}$$

in $U^h = Q_1^D \times RT_0^N$. The standard finite element implementation of this method solves the following variational equation: *seek* $\{p^h,\mathbf{u}^h\} \in Q_1^D \times RT_0^N$ *such that*

$$\left\{\begin{array}{l} \displaystyle\int_\Omega (\nabla p^h + \Theta_1^{-1}\mathbf{u}^h)\Theta_1(\nabla q^h + \Theta_1^{-1}\mathbf{v}^h)dx \\ \qquad\qquad + \displaystyle\int_\Omega (\nabla\cdot\mathbf{u}^h + \sigma\Theta_0 p^h)\Theta_0^{-1}(\nabla\cdot\mathbf{v}^h + \sigma\Theta_0 q^h)dx \\ \displaystyle = \int_\Omega f\Theta_0^{-1}(\nabla\cdot\mathbf{v}^h + \sigma\Theta_0 q^h)dx \qquad \forall q^h \in Q_1^D,\ \forall \mathbf{v}^h \in RT_0^N\,. \end{array}\right. \tag{4.3}$$

The following theorem from [8] provides additional information about the standard least-squares method. It was used in [8] to conclude that (4.3) is locally conservative.

THEOREM 4.1. *Assume that the reaction term is present in (1.1), i.e.,* $\sigma = 1$. *Then, the least-squares equation (4.3) decouples into independent problems for the velocity: seek* $\mathbf{u}^h \in RT_0^N$ *such that*

$$\int_\Omega \mathbf{u}^h\Theta^{-1}\mathbf{v}^h\, dx + \int_\Omega \nabla\cdot\mathbf{u}^h\Theta_0^{-1}\nabla\cdot\mathbf{v}^h\, dx = \int_\Omega f\Theta_0^{-1}\nabla\cdot\mathbf{v}^h\, dx \quad \forall \mathbf{v}^h \in RT_0^N\,; \tag{4.4}$$

and the pressure: seek $p^h \in Q_1^D$ *such that*

$$\int_\Omega \nabla p^h\Theta_1\nabla q^h\, dx + \int_\Omega p^h\Theta_0 q^h\, dx = \int_\Omega f q^h\, dx \quad \forall q^h \in Q_1^D\,. \tag{4.5}$$

If the grid is such that the analytic divergence is a surjective map $RT_0 \mapsto Q_0$, *then the solution of the weak problem (4.4) coincides with the velocity approximation in the mixed method (4.1).*

For proof of this theorem we refer to [8]. On the positive side, Theorem 4.1 implies that for problems with a reaction term the deterioration of accuracy should not spread to the pressure approximation. This follows from the fact that equation (4.5) defines the Ritz-Galerkin method for (1.1) which retains optimal orders of convergence on general quadrilateral grids; see [13].

On the negative side, for non-affine quadrilateral elements the analytic divergence does not map RT_0 onto Q_0 (see Remark 2) and so, solution of (4.4) will not coincide with the velocity approximation in the mixed method. Considering that Theorem 5.1 below will show that the mixed method produces accurate velocities, this spells potential trouble for the least-squares velocity.

Of course, in the absence of a reaction term ($\sigma = 0$) the least-squares equation remains coupled. In this case we can expect deterioration of accuracy in both variables. Numerical tests in [4] confirm this conjecture. Section 6 will provide further computational evidence to corroborate these conclusions.

4.2. Reformulated methods. We obtain mimetic reformulations of (4.1) and (4.3) by swapping the analytic divergence with DIV. The reformulated mixed method is: *seek* $\mathbf{u}^h \in RT_0^N$ *and* $p^h \in Q_0$ *such that*

$$\left\{\begin{array}{ll} \displaystyle\int_\Omega \mathbf{u}^h \Theta_1^{-1} \mathbf{v}^h \, dx - \int_\Omega p^h \mathsf{DIV}(\mathbf{v}^h)\, dx = 0 & \forall \mathbf{v}^h \in RT_0^N \\ \displaystyle\int_\Omega \mathsf{DIV}(\mathbf{u}^h) q^h \, dx + \sigma \int_\Omega p^h \Theta_0 q^h \, dx = \int_\Omega f q^h \, dx & \forall q^h \in Q_0. \end{array}\right. \tag{4.6}$$

We make the usual identifications

$$a^h(\mathbf{u}^h, \mathbf{v}^h) = \int_\Omega \mathbf{u}^h \Theta_1^{-1} \mathbf{v}^h \, dx \quad \text{and} \quad b^h(\mathbf{u}^h, p^h) = \int_\Omega p^h \mathsf{DIV}(\mathbf{u}^h)\, dx\,.$$

Note that $a^h(\cdot,\cdot)$ and $b^h(\cdot,\cdot)$ are defined only for finite element functions.

Reformulation of the least-squares method is: *seek* $\{p^h, \mathbf{u}^h\} \in Q_1^D \times RT_0^N$ *such that*

$$\left\{\begin{array}{l} \displaystyle\int_\Omega (\nabla p^h + \Theta_1^{-1}\mathbf{u}^h)\Theta_1(\nabla q^h + \Theta_1^{-1}\mathbf{v}^h) dx \\ \qquad\qquad + \displaystyle\int_\Omega (\mathsf{DIV}(\mathbf{u}^h) + \sigma\Theta_0 p^h)\Theta_0^{-1}(\mathsf{DIV}(\mathbf{v}^h) + \sigma\Theta_0 q^h) dx \\ \displaystyle = \int_\Omega f\Theta_0^{-1}(\mathsf{DIV}(\mathbf{v}^h) + \sigma\Theta_0 q^h) dx \qquad \forall q^h \in Q_1^D,\ \forall \mathbf{v}^h \in RT_0^N\,. \end{array}\right. \tag{4.7}$$

REMARK 4. *An existing finite element program for the standard mixed or the least-squares method can be trivially converted to its mimetic reformulation by changing just a few lines of code. From (3.1), (2.2), and* $\mu(\hat\kappa) = 4$ *it follows that*

$$\mathsf{DIV}(\mathbf{u}_{\boldsymbol{f}})|_\kappa = \frac{\sigma_{\boldsymbol{f}}}{\mu(\kappa)} = \frac{\sigma_{\boldsymbol{f}}}{4\det(D\Phi(0,0))}\,.$$

As a result, the conversion to mimetic reformulations amounts to replacing multiple calls to the function that computes $\nabla\cdot\mathbf{u}_{\boldsymbol{f}}(\boldsymbol{x})$ *at quadrature points, along with the computation of* $\det D\Phi$ *at those points, by a single call to compute* $\det(D\Phi(0,0))$ *combined with a few Boolean operations related to the orientation choice* $\sigma_{\boldsymbol{f}}$.

REMARK 5. *An alternative approach that also restores the first-order convergence in the divergence error has been proposed in [23]. The idea is to "correct" the standard*

RT_0 basis on $\hat{\kappa}$ so that the basis functions on any $\kappa \in \mathcal{T}_h$ have constant divergence. Correction is effected by adding a vector field defined with the help of $\det D\Phi_\kappa$ *which makes the reference basis dependent upon the elements in $\mathcal{T}_h$. This should be contrasted with our approach where the definition of the RT_0 basis on $\hat{\kappa}$ is unchanged and remains independent of $\kappa \in \mathcal{T}_h$; instead one changes the definition of the divergence operator on κ. Connection between a mixed method implemented with the modified RT_0 space and a mimetic finite difference scheme for (1.1) is shown in [10].*

5. Properties of reformulated methods. This section examines stability and convergence of the reformulated methods. We begin with the analysis of the reformulated mixed method.

5.1. The mixed method. The following theorem shows that (4.1) and (4.6) are equivalent.

THEOREM 5.1. *The standard mixed method (4.1) and its mimetic reformulation (4.6) give rise to identical linear systems of equations for the unknown coefficients of $\mathbf{u}^h \in RT_0^N$ and $p^h \in Q_0$, i.e., their solutions coincide.*

Proof. The mixed problem (4.1) and its mimetic reformulation (4.6) reduce to the linear systems of equations

$$\begin{bmatrix} \mathbf{M_u} & \mathbf{D}^T \\ \mathbf{D} & \mathbf{M}_p \end{bmatrix} \begin{bmatrix} \vec{\mathbf{u}} \\ \vec{p} \end{bmatrix} = \begin{bmatrix} \vec{0} \\ \vec{f} \end{bmatrix} \quad \text{and} \quad \begin{bmatrix} \mathbf{M_u} & \widetilde{\mathbf{D}}^T \\ \widetilde{\mathbf{D}} & \mathbf{M}_p \end{bmatrix} \begin{bmatrix} \vec{\mathbf{u}} \\ \vec{p} \end{bmatrix} = \begin{bmatrix} \vec{0} \\ \vec{f} \end{bmatrix},$$

respectively, for the unknown coefficients $\vec{\mathbf{u}}$, $\vec{p}$ of $\mathbf{u}^h$ and p^h. Here $\mathbf{M_u}$ and $\mathbf{M}_p$ are the consistent mass matrices for RT_0 and Q_0 finite element spaces, respectively. The matrices $\mathbf{D}$ and $\widetilde{\mathbf{D}}$ are given by their respective entries

$$\mathbf{D}_{\boldsymbol{f},\kappa} = \int_\Omega p_\kappa \nabla \cdot \mathbf{u}_{\boldsymbol{f}}\, dx \quad \text{and} \quad \widetilde{\mathbf{D}}_{\boldsymbol{f},\kappa} = \int_\Omega p_\kappa \mathsf{DIV}(\mathbf{u}_{\boldsymbol{f}})\, dx\,, \quad \boldsymbol{f} \in \mathcal{F}_h,\ \kappa \in \mathcal{T}_h\,.$$

The theorem will follow if we can show that $\mathbf{D}_{\boldsymbol{f},\kappa} = \widetilde{\mathbf{D}}_{\boldsymbol{f},\kappa}$. Let κ be fixed and $\boldsymbol{f}$ one of its faces. The basis function $p_\kappa = 1/\mu(\kappa)$ is constant on κ and $p_\kappa = 0$ on all other elements. Therefore, using (3.5) from Lemma 3.3 it follows that

$$\begin{aligned} \mathbf{D}_{\boldsymbol{f},\kappa} &= \int_\Omega p_\kappa \nabla \cdot \mathbf{u}_{\boldsymbol{f}}\, dx = \frac{1}{\mu(\kappa)} \int_\kappa \nabla \cdot \mathbf{u}_{\boldsymbol{f}}\, dx \\ &= \frac{1}{\mu(\kappa)} \int_\kappa \mathsf{DIV}(\mathbf{u}_{\boldsymbol{f}})\, dx = \int_\Omega p_\kappa \mathsf{DIV}(\mathbf{u}_{\boldsymbol{f}})\, dx = \quad \widetilde{\mathbf{D}}_{\boldsymbol{f},\kappa}\,. \end{aligned}$$

□

REMARK 6. *D. Boffi brought to our attention a similar equivalence result [9] for two modifications of a primal finite element method for the Maxwell's eigenvalue problem*[8] *defined by using a local L^2 projection and reduced integration, respectively. From (3.3) in Lemma 3.1 $\mathsf{DIV}\big(\mathbf{u}^h\big) = \mathcal{I}_{Q_0}(\nabla \cdot \mathbf{u}^h)$ for all $\mathbf{u}^h \in RT_0$, from where it follows that the first approach of [9] is equivalent to our mimetic reformulation.*

In light of this theorem we could in principle skip a formal stability analysis of the reformulated mixed method because we already know that the discrete system in the standard mixed method is well-behaved. However, a separate stability proof

[8] Finite element solution of this problem in two dimensions requires "rotated" *RT* elements which suffer from the same accuracy problems as standard *RT* elements on non-affine quadrilateral grids.

for (4.6) will be very convenient for the error estimates where we will work with the discrete norm $\|\mathbf{u}^h\|_{\mathsf{DIV}} = (\|\mathbf{u}^h\|_0^2 + \|\mathsf{DIV}(\mathbf{u}^h)\|_0^2)^{1/2}$. The proofs are stated for the case $\sigma = 0$. The extension to $\sigma = 1$ is straightforward.

LEMMA 5.2. *Let* $Z^h = \{\mathbf{u}^h \in RT_0 \,|\, \mathsf{DIV}(\mathbf{u}^h) = 0\}$ *denote the null-space of* DIV. *The form* $a^h(\cdot,\cdot)$ *is coercive on* $Z^h \times Z^h$*:*

$$C_a\|\mathbf{v}^h\|^2 \le a^h(\mathbf{v}^h,\mathbf{v}^h) \quad \forall \mathbf{v}^h \in Z^h\,. \tag{5.1}$$

The form $b^h(\cdot,\cdot)$ *satisfies a discrete inf-sup condition:*

$$\sup_{\mathbf{v}^h\in RT_0} \frac{b^h(\mathbf{v}^h,p^h)}{\|\mathbf{v}^h\|_{\mathsf{DIV}}} \ge C_b\|p^h\|_0 \quad \forall p^h \in Q_0\,. \tag{5.2}$$

Proof. The first statement is a direct consequence of the definition of Z^h and condition (1.2) on the tensor Θ_1. To prove the inf-sup condition we proceed as follows. Let $p^h \in Q_0$ be arbitrary. From Lemma 3.2 we know that there exists a $\mathbf{u}_p^h \in RT_0$ such that (3.4) holds. Therefore,

$$\sup_{\mathbf{v}^h\in RT_0} \frac{b^h(\mathbf{v}^h,p^h)}{\|\mathbf{v}^h\|_{\mathsf{DIV}}} \ge \frac{b^h(\mathbf{u}_p^h,p^h)}{\|\mathbf{u}_p^h\|_{\mathsf{DIV}}} \ge \frac{\|p^h\|_0^2}{\|\mathbf{u}_p^h\|_{\mathsf{DIV}}} \ge C\|p^h\|_0\,.$$

□

Lemma 5.2 directly implies the following stability result.

THEOREM 5.3. *Define the discrete bilinear operator*

$$Q^h(\mathbf{u}^h,p^h;\mathbf{v}^h,q^h) = a^h(\mathbf{u}^h,\mathbf{v}^h) - b^h(\mathbf{v}^h,p^h) + b^h(\mathbf{u}^h,q^h)\,.$$

There exists a positive constant C_Q *such that*

$$\sup_{(\mathbf{v}^h,q^h)\in RT_0^N\times Q_0} \frac{Q^h(\mathbf{u}^h,p^h;\mathbf{v}^h,q^h)}{\|\mathbf{v}^h\|_{\mathsf{DIV}} + \|q^h\|_0} \ge C_Q\left(\|\mathbf{u}^h\|_{\mathsf{DIV}} + \|p^h\|_0\right)\,. \tag{5.3}$$

We can now prove optimal error estimates for (4.6).

THEOREM 5.4. *Assume that (2.1) holds for the finite element partition* $\mathcal{T}_h$ *and that the exact solution of (1.1) is such that* $p \in H_D^1(\Omega)$ *and* $\mathbf{u} \in H_N(\mathrm{div},\Omega) \cap (H^2(\Omega))^2$*. Solution of the reformulated mixed problem (4.6) satisfies the error bound*

$$\|\nabla\cdot\mathbf{u} - \mathsf{DIV}(\mathbf{u}^h)\|_0 + \|\mathbf{u}-\mathbf{u}^h\|_0 + \|p-p^h\|_0 \le Ch\left(\|\mathbf{u}\|_2 + \|p\|_1\right)\,. \tag{5.4}$$

Proof. To avoid tedious technical details, we limit the proof to the case $\Theta_1 = \mathbb{I}$. We begin by splitting the left hand side in (5.4) into interpolation error and discrete error:

$$\begin{aligned}
&\|\nabla\cdot\mathbf{u} - \mathsf{DIV}(\mathbf{u}^h)\|_0 + \|\mathbf{u}-\mathbf{u}^h\|_0 + \|p-p^h\|_0\\
&\quad\le \left(\|\nabla\cdot\mathbf{u} - \mathsf{DIV}\mathcal{I}(\mathbf{u})\|_0 + \|\mathbf{u}-\mathcal{I}\mathbf{u}\|_0 + \|p-\mathcal{I}p\|_0\right)\\
&\qquad + \left(\|\mathsf{DIV}\mathcal{I}(\mathbf{u}) - \mathsf{DIV}(\mathbf{u}^h)\|_0 + \|\mathcal{I}\mathbf{u}-\mathbf{u}^h\|_0 + \|\mathcal{I}p-p^h\|_0\right) = E_{\mathcal{I}} + E_h\,.
\end{aligned}$$

The next step is to estimate the discrete error E_h in terms of the interpolation error $E_{\mathcal{I}}$. We make use of the fact that for $(\mathbf{v}^h,q^h) \in RT_0^N \times Q_0$

$$\int_\Omega \mathbf{u}^h\mathbf{v}^h\,dx - \int_\Omega p^h\mathsf{DIV}(\mathbf{v}^h)\,dx \;=\; 0 \;=\; \int_\Omega \mathbf{u}\mathbf{v}^h\,dx - \int_\Omega p\nabla\cdot\mathbf{v}^h\,dx \tag{5.5}$$

and

$$\int_\Omega q^h \mathsf{DIV}(\mathbf{u}^h)\,dx \;=\; \int_\Omega f q^h\,dx \;=\; \int_\Omega q^h \nabla\cdot\mathbf{u}\,dx\,. \tag{5.6}$$

For brevity we switch to inner product notation. Adding and subtracting $\mathcal{I}\mathbf{u}$ and $\mathcal{I}p$ in (5.5) we obtain

$$\left(\mathbf{u}-\mathcal{I}\mathbf{u},\mathbf{v}^h\right)+\left(\mathcal{I}\mathbf{u}-\mathbf{u}^h,\mathbf{v}^h\right)-\left(p-\mathcal{I}p,\nabla\cdot\mathbf{v}^h\right)-\left(\mathcal{I}p,\nabla\cdot\mathbf{v}^h\right)+\left(p^h,\mathsf{DIV}(\mathbf{v}^h)\right)=0\,.$$

As $\mathcal{I}p$ is constant, by Lemma (3.3) we can replace $\left(\mathcal{I}p,\nabla\cdot\mathbf{v}^h\right)$ by $\left(\mathcal{I}p,\mathsf{DIV}(\mathbf{v}^h)\right)$, thus

$$\left(\mathbf{u}^h-\mathcal{I}\mathbf{u},\mathbf{v}^h\right)+\left(\mathcal{I}p-p^h,\mathsf{DIV}(\mathbf{v}^h)\right)=\left(\mathbf{u}-\mathcal{I}\mathbf{u},\mathbf{v}^h\right)+\left(\mathcal{I}p-p,\nabla\cdot\mathbf{v}^h\right). \tag{5.7}$$

Adding and subtracting $\mathcal{I}(\nabla\cdot\mathbf{u})$ in (5.6) yields

$$\left(\nabla\cdot\mathbf{u}-\mathcal{I}(\nabla\cdot\mathbf{u}),q^h\right)+\left(\mathcal{I}(\nabla\cdot\mathbf{u})-\mathsf{DIV}(\mathbf{u}^h),q^h\right)=0.$$

Using CDP,

$$\left(\mathsf{DIV}(\mathbf{u}^h-\mathcal{I}\mathbf{u}),q^h\right)=\left(\nabla\cdot\mathbf{u}-\mathsf{DIV}(\mathcal{I}\mathbf{u}),q^h\right). \tag{5.8}$$

Substituting $(\mathbf{u}^h-\mathcal{I}\mathbf{u},\mathcal{I}p-p^h)$ into the inf-sup result (5.3), we get

$$\begin{aligned}
&Q^h(\mathbf{u}^h-\mathcal{I}\mathbf{u},\mathcal{I}p-p^h;\mathbf{v}^h,q^h)\\
&\qquad\geq C_Q\left(\|\mathbf{u}^h-\mathcal{I}\mathbf{u}\|_0+\|\mathsf{DIV}(\mathbf{u}^h-\mathcal{I}\mathbf{u})\|_0+\|p^h-\mathcal{I}p\|_0\right)\\
&\qquad\quad\times\left(\|\mathbf{v}^h\|_0+\|\mathsf{DIV}(\mathbf{v}^h)\|_0+\|q^h\|_0\right)\,.
\end{aligned}$$

On the other hand, due to the definition of Q^h, (5.7), (5.8), Cauchy inequalities, and Lemma 3.4,

$$\begin{aligned}
&Q^h(\mathbf{u}^h-\mathcal{I}\mathbf{u},\mathcal{I}p-p^h;\mathbf{v}^h,q^h)\\
&\qquad=\left(\mathbf{u}-\mathcal{I}\mathbf{u},\mathbf{v}^h\right)+\left(\mathcal{I}p-p,\nabla\cdot\mathbf{v}^h\right)+\left(\nabla\cdot\mathbf{u}-\mathsf{DIV}(\mathcal{I}\mathbf{u}),q^h\right)\\
&\qquad\leq\left(\|\mathbf{u}-\mathcal{I}\mathbf{u}\|_0+\|p-\mathcal{I}p\|_0+\|\nabla\cdot\mathbf{u}-\mathsf{DIV}(\mathcal{I}\mathbf{u})\|_0\right)\\
&\qquad\quad\times\left(\|\mathbf{v}^h\|_0+C_D\|\mathsf{DIV}(\mathbf{v}^h)\|_0+\|q^h\|_0\right),
\end{aligned}$$

for a positive constant C_D. It is safe to assume $C_D\geq 1$ (without loss of generality), thus $\left(\|\mathbf{v}^h\|_0+C_D\|\mathsf{DIV}(\mathbf{v}^h)\|_0+\|q^h\|_0\right)\leq C_D\left(\|\mathbf{v}^h\|_0+\|\mathsf{DIV}(\mathbf{v}^h)\|_0+\|q^h\|_0\right)$, which, combined with the previous two estimates of Q^h, yields

$$\begin{aligned}
E_h&=\|\mathbf{u}^h-\mathcal{I}\mathbf{u}\|_0+\|\mathsf{DIV}(\mathbf{u}^h-\mathcal{I}\mathbf{u})\|_0+\|p^h-\mathcal{I}p\|_0\\
&\leq\frac{C_D}{C_Q}\left(\|\mathbf{u}-\mathcal{I}\mathbf{u}\|_0+\|p-\mathcal{I}p\|_0+\|\nabla\cdot\mathbf{u}-\mathsf{DIV}(\mathcal{I}\mathbf{u})\|_0\right)=\frac{C_D}{C_Q}E_{\mathcal{I}}.
\end{aligned}$$

Therefore,

$$\|\nabla\cdot\mathbf{u}-\mathsf{DIV}(\mathbf{u}^h)\|_0+\|\mathbf{u}-\mathbf{u}^h\|_0+\|p-p^h\|_0\leq\left(1+\frac{C_D}{C_Q}\right)E_{\mathcal{I}}. \tag{5.9}$$

The remainder of the proof follows from CDP, (2.11), and (2.12). We have

$$\|\nabla\cdot\mathbf{u}-\mathsf{DIV}(\mathcal{I}\mathbf{u})\|_0=\|\nabla\cdot\mathbf{u}-\mathcal{I}(\nabla\cdot\mathbf{u})\|_0\le Ch\|\nabla\cdot\mathbf{u}\|_1,$$

and

$$\|\mathbf{u}-\mathcal{I}\mathbf{u}\|_0+\|p-\mathcal{I}p\|_0\le Ch\left(\|\mathbf{u}\|_1+\|p\|_1\right),$$

i.e.,

$$E_{\mathcal{I}}\le Ch\left(\|\nabla\cdot\mathbf{u}\|_1+\|\mathbf{u}\|_1+\|p\|_1\right)\le Ch\left(\|\mathbf{u}\|_2+\|p\|_1\right),$$

which establishes (5.4).
□

REMARK 7. *The presence of the constant C_D in (5.9) indicates that the size of the approximation error is directly related to assumption (2.1) on the shape-regularity of the finite element partition $\mathcal{T}_h$.*

5.2. The least-squares method. It is easy to see that the equivalence result of Theorem 5.1 cannot be extended to the least-squares method. To convince ourselves that the mimetic reformulation (4.7) of this method is genuinely different from its standard version (4.3) let us examine the term

$$\int_\Omega(\mathsf{DIV}(\mathbf{u}^h)+\sigma\Theta_0p^h)\Theta_0^{-1}(\mathsf{DIV}(\mathbf{v}^h)+\sigma\Theta_0q^h)dx$$

from (4.7). It is clear that for the same reasons as stated in Remark 2, on a non-affine quadrilateral element

$$\int_\Omega\mathsf{DIV}(\mathbf{u}^h)\Theta_0^{-1}\mathsf{DIV}(\mathbf{v}^h)dx\ne\int_\Omega\nabla\cdot\mathbf{u}^h\Theta_0^{-1}\nabla\cdot\mathbf{v}^hdx.$$

The cross terms also don't match because in the least-squares method $p^h\in Q_1$ is not constant and cannot be pulled out of the integral as in Theorem 5.1. Thus,

$$\int_\Omega q^h\mathsf{DIV}(\mathbf{u}^h)dx\ne\int_\Omega q^h\nabla\cdot\mathbf{u}^hdx\,.$$

Another difference between the two versions of the least-squares method is that the splitting in Theorem 4.1 does not extend to the mimetic reformulation (4.7). This would require the discrete Green's identity

$$\int_\Omega p^h\mathsf{DIV}(\mathbf{u}^h)\,dx+\int_\Omega\mathbf{u}^h\nabla p^h\,dx=0\quad\forall\mathbf{u}^h\in RT_0^N;\ \ \forall p^h\in Q_1^D,$$

which in general does not hold. Therefore, velocity computed by (4.7) is not locally conservative in the sense described in [8]. This can be fixed by using the flux-correction procedure defined in [8].

The following theorem asserts stability of the reformulated least-squares method.

THEOREM 5.5. *Assume that (2.1) holds. There is a positive constant C such that*

$$\begin{aligned}&C\left(\|\mathsf{DIV}(\mathbf{u}^h)\|_0+\|\mathbf{u}^h\|_0+\|p^h\|_1\right)\\&\qquad\le\|\Theta_0^{-1/2}\left(\mathsf{DIV}(\mathbf{u}^h)+\Theta_0p^h\right)\|_0+\|\Theta_1^{1/2}(\nabla p^h+\Theta_1^{-1}\mathbf{u}^h)\|_0\,.\end{aligned}\tag{5.10}$$

for every $\mathbf{u}^h \in RT_0^N$ *and* $p^h \in Q_1^D$.

Proof. To avoid simple but tedious technical details we state the proof for $\Theta_1 = \mathbb{I}$ and $\Theta_0 = 1$. In this case, the right hand side in (5.10) expands into

$$\begin{aligned}\|\mathsf{DIV}(\mathbf{u}^h) + p^h\|_0^2 + \|\nabla p^h + \mathbf{u}^h\|_0^2 = 2\left(\int_\Omega p^h \mathsf{DIV}(\mathbf{u}^h)\,dx + \int_\Omega \mathbf{u}^h \nabla p^h\,dx\right)\\ +\|\mathbf{u}^h\|_0^2 + \|\mathsf{DIV}(\mathbf{u}^h)\|_0^2 + \|p^h\|_0^2 + \|\nabla p^h\|_0^2\,.\end{aligned}$$

We switch to inner product notation. Adding and subtracting the projection of p^h onto Q_0, using Green's identity, equation (3.5) in Lemma 3.3, and Cauchy's inequality:

$$\begin{aligned}&\big(\mathsf{DIV}(\mathbf{u}^h), p^h\big) + \big(\nabla p^h, \mathbf{u}^h\big)\\ &\quad= \big(\mathsf{DIV}(\mathbf{u}^h), p^h - \mathcal{I}_{Q_0} p^h\big) + \big(\mathsf{DIV}(\mathbf{u}^h), \mathcal{I}_{Q_0} p^h\big) - \big(\nabla\cdot\mathbf{u}^h, p^h\big)\\ &\quad= \big(\mathsf{DIV}(\mathbf{u}^h), p^h - \mathcal{I}_{Q_0} p^h\big) + \big(\nabla\cdot\mathbf{u}^h, \mathcal{I}_{Q_0} p^h - p^h\big)\\ &\quad\le \|\mathsf{DIV}(\mathbf{u}^h)\|_0 \|p^h - \mathcal{I}_{Q_0} p^h\|_0 + \|\nabla\cdot\mathbf{u}^h\|_0 \|p^h - \mathcal{I}_{Q_0} p^h\|_0\,.\end{aligned}$$

Using (3.6) from Lemma 3.4, the approximation result (2.11), and the inequality $2ab \le a^2 + b^2$

$$\begin{aligned}&2\left(\big(\mathsf{DIV}(\mathbf{u}^h), p^h\big) + \big(\nabla p^h, \mathbf{u}^h\big)\right)\\ &\quad\le 2(1+C_D)Ch\|\mathsf{DIV}(\mathbf{u}^h)\|_0\|\nabla p^h\|_0 \le (1+C_D)Ch\left(\|\mathsf{DIV}(\mathbf{u}^h)\|_0^2 + \|\nabla p^h\|_0^2\right)\end{aligned}$$

As a result, for sufficiently small h

$$\begin{aligned}&\|\mathsf{DIV}(\mathbf{u}^h) + p^h\|_0^2 + \|\nabla p^h + \mathbf{u}^h\|_0^2\\ &\quad\ge (1-(1+C_D)Ch)\left(\|\mathbf{u}^h\|_0^2 + \|\mathsf{DIV}(\mathbf{u}^h)\|_0^2 + \|p^h\|_0^2 + \|\nabla p^h\|_0^2\right)\\ &\quad\ge \frac{1}{2}\left(\|\mathbf{u}^h\|_0^2 + \|\mathsf{DIV}(\mathbf{u}^h)\|_0^2 + \|p^h\|_1^2\right).\end{aligned}$$

□

Theorem 5.5 in conjunction with the Lax-Milgram lemma implies that the reformulated least-squares problem has a unique solution. Using this theorem we can also prove optimal error estimates for the solution of (4.7).

THEOREM 5.6. *Assume that (2.1) holds for the finite element partition* $\mathcal{T}_h$ *and that the exact solution of (1.1) is such that* $p \in H_D^1(\Omega)\cap H^2(\Omega)$ *and* $\mathbf{u} \in H_N(\mathrm{div}\,,\Omega)\cap (H^2(\Omega))^2$. *Solution of the reformulated least-squares problem (4.7) satisfies the error bound*

$$\|\nabla\cdot\mathbf{u} - \mathsf{DIV}(\mathbf{u}^h)\|_0 + \|\mathbf{u} - \mathbf{u}^h\|_0 + \|p - p^h\|_1 \le Ch\left(\|p\|_2 + \|\mathbf{u}\|_2\right) \tag{5.11}$$

Proof. For clarity we state the proof using the same setting as in the proof of Theorem 5.5. We begin by splitting the left hand side in (5.11) into interpolation error and discrete error:

$$\begin{aligned}&\|\nabla\cdot\mathbf{u} - \mathsf{DIV}(\mathbf{u}^h)\|_0 + \|\mathbf{u} - \mathbf{u}^h\|_0 + \|p - p^h\|_1\\ &\quad\le \left(\|\nabla\cdot\mathbf{u} - \mathsf{DIV}\mathcal{I}(\mathbf{u})\|_0 + \|\mathbf{u} - \mathcal{I}\mathbf{u}\|_0 + \|p - \mathcal{I}p\|_1\right)\\ &\qquad+ \left(\|\mathsf{DIV}\mathcal{I}(\mathbf{u}) - \mathsf{DIV}(\mathbf{u}^h)\|_0 + \|\mathcal{I}\mathbf{u} - \mathbf{u}^h\|_0 + \|\mathcal{I}p - p^h\|_1\right) = E_{\mathcal{I}} + E_h\,.\end{aligned}$$

The next step is to estimate E_h in terms of the interpolation error. For this purpose, we use that $f = \nabla \cdot \mathbf{u} + p$ and $0 = \nabla p + \mathbf{u}$ to write (4.7) as

$$\begin{aligned}\big(\mathsf{DIV}(\mathbf{u}^h) + p^h, \mathsf{DIV}(\mathbf{v}^h) + q^h\big) + \big(\nabla p^h + \mathbf{u}^h, \nabla q^h + \mathbf{v}^h\big)\\ = \big(\nabla \cdot \mathbf{u} + p, \mathsf{DIV}(\mathbf{v}^h) + q^h\big) + \big(\nabla p + \mathbf{u}, \nabla q^h + \mathbf{v}^h\big)\ .\end{aligned}$$

Subtracting the interpolants of p and $\mathbf{u}$ from both sides of this identity, and using Cauchy's inequality gives

$$\begin{aligned}&\big(\mathsf{DIV}(\mathbf{u}^h - \mathcal{I}\mathbf{u}) + p^h - \mathcal{I}p, \mathsf{DIV}(\mathbf{v}^h) + q^h\big) + \big(\nabla(p^h - \mathcal{I}p) + \mathbf{u}^h - \mathcal{I}\mathbf{u}, \nabla q^h + \mathbf{v}^h\big)\\ &= \big(\nabla\cdot\mathbf{u} - \mathsf{DIV}(\mathcal{I}\mathbf{u}) + p - \mathcal{I}p, \mathsf{DIV}(\mathbf{v}^h) + q^h\big) + \big(\nabla(p - \mathcal{I}p) + \mathbf{u} - \mathcal{I}\mathbf{u}, \nabla q^h + \mathbf{v}^h\big)\\ &\le C(\|\nabla\cdot\mathbf{u} - \mathsf{DIV}(\mathcal{I}\mathbf{u})\|_0 + \|\mathbf{u} - \mathcal{I}\mathbf{u}\|_0 + \|p - \mathcal{I}p\|_1)\ \big(\|\mathsf{DIV}(\mathbf{v}^h)\|_0 + \|\mathbf{v}^h\|_0 + \|q^h\|_1\big)\\ &\le CE_{\mathcal{I}} \times \big(\|\mathsf{DIV}(\mathbf{v}^h)\|_0 + \|\mathbf{v}^h\|_0 + \|q^h\|_1\big)\ .\end{aligned}$$

Then we set $\mathbf{v}^h = \mathbf{u}^h - \mathcal{I}\mathbf{u}$, $q^h = p^h - \mathcal{I}p$ and use the stability bound (5.10):

$$\begin{aligned}E_h^2 \le C\ &\big(\mathsf{DIV}(\mathbf{u}^h - \mathcal{I}\mathbf{u}) + p^h - \mathcal{I}p, \mathsf{DIV}(\mathbf{u}^h - \mathcal{I}\mathbf{u}) + p^h - \mathcal{I}p\big)\\ &+ \big(\nabla(p^h - \mathcal{I}p) + \mathbf{u}^h - \mathcal{I}\mathbf{u}, \nabla(p^h - \mathcal{I}p) + \mathbf{u}^h - \mathcal{I}\mathbf{u}\big) \le CE_{\mathcal{I}} \times E_h\,.\end{aligned}$$

Therefore, $E_h \le CE_{\mathcal{I}}$ and

$$\|\nabla \cdot \mathbf{u} - \mathsf{DIV}(\mathbf{u}^h)\|_0 + \|\mathbf{u} - \mathbf{u}^h\|_0 + \|p - p^h\|_1 \le (1 + C)E_{\mathcal{I}}\,.$$

To complete the proof we estimate $E_{\mathcal{I}}$ as follows. Using CDP (3.3) and (2.11),

$$\|\nabla \cdot \mathbf{u} - \mathsf{DIV}\mathcal{I}(\mathbf{u})\|_0 = \|\nabla \cdot \mathbf{u} - \mathcal{I}(\nabla \cdot \mathbf{u})\|_0 \le Ch\|\nabla \cdot \mathbf{u}\|_1\,,$$

while from (2.12) and (2.13) we have that

$$\|\mathbf{u} - \mathcal{I}\mathbf{u}\|_0 + \|p - \mathcal{I}p\|_1 \le Ch\,(\|\mathbf{u}\|_1 + \|p\|_2)\ ,$$

Therefore,

$$E_{\mathcal{I}} \le Ch\,(\|p\|_2 + \|\mathbf{u}\|_2)\ .$$

This establishes (5.11). □

6. Numerical results. Computational experiments in this section illustrate the properties of standard and reformulated finite element methods using three different partitions of $\Omega = [0, 1]^2$ into quadrilateral elements; see Fig. 6.1. We refer to the leftmost partition in this figure as the "trapezoidal grid". This grid was used by Arnold et. al. [4] to demonstrate loss of accuracy in div-conforming elements and is characterized by a high-degree of "non-affinity". The middle partition corresponds to a randomly perturbed[9] uniform grid which provides a more realistic example of a

[9]This grid was suggested by one of the anonymous referees and is defined as follows. We start with a uniform partition of Ω into square elements with side lengths h and draw a circle of radius $h/4$ around each node. All internal nodes are then randomly repositioned inside these circles, corner nodes are held fixed and the rest of the nodes on the boundary are moved randomly along the sides of Ω within $\pm h/4$ of their original locations.

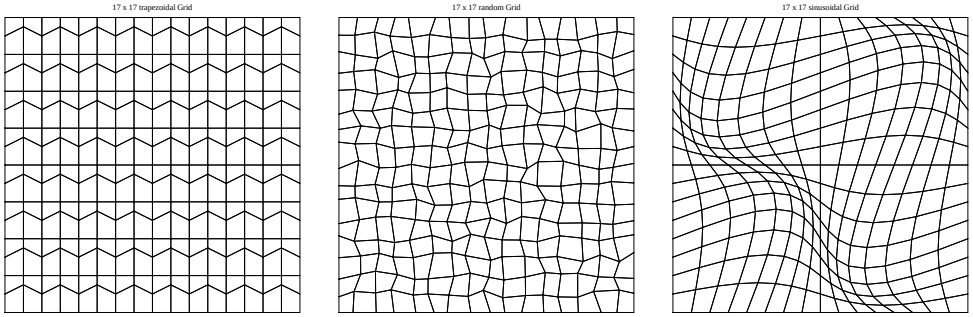

FIG. 6.1. *Quadrilateral grids used in the computational experiments. From left to right: trapezoidal grid [4], randomly perturbed grid and sinusoidal grid [20].*

highly non-affine quadrilateral grid. The rightmost partition in Fig. 6.1 is taken from [20] and provides an example of a smooth non-orthogonal grid[10] which may become quite distorted while retaining "near-affinity" of most of its quadrilateral elements. This grid is used to underscore the fact that the root cause for the loss of convergence is non-afffinity of the grid rather than the level of its distortion.

We show that on the first two partitions, i.e., on trapezoidal and random grids:

- the natural divergence of the velocity approximation in the standard mixed method is first-order accurate, i.e., it is optimally accurate;
- the deterioration of accuracy in the least-squares method does not spread to the pressure approximation if the reaction term is present, but that the velocity approximation is worse than in the mixed method;
- without the reaction term, the deterioration of accuracy affects all variables in the least-squares method;
- the mimetic reformulation of the least-squares method solves all these problems and yields optimally accurate pressure and velocity approximations.

As far as the last partition is concerned, we show that thanks to the almost affine nature of the sinusoidal grid there's virtually no degradation of accuracy in mixed and least-squares methods.

The linear systems are assembled using 2×2 Gauss quadrature and solved "exactly" using direct solvers. The order of convergence study solves (1.1) with $\Gamma_N = \emptyset$,

$$\Theta_1 = \begin{bmatrix} \exp((x+y/2)/2) & \sin(2\pi x) \\ \sin(2\pi x) & \exp((x/2+y)/2) \end{bmatrix}, \quad \Theta_0 = 1\,,$$

and the right hand side and boundary data generated from the manufactured solution

$$p = -\exp(x)\sin(y), \quad \text{and} \quad \mathbf{u} = -\Theta_1 \nabla p\,.$$

Orders of convergence are estimated using data on 33×33, 65×65 and 129×129 grids with 1024, 4096 and 16384 elements, respectively.

The maximum anisotropy of Θ_1 is is attained at the top right corner of Ω and equals $4\exp(3/2) \approx 18$. The non-constant full tensor permeability is used only in

[10] The nodal positions in this grid are defined by

$$x(\xi,\eta,t) = \xi + \alpha(t)\sin(2\pi\xi)\sin(2\pi\eta)\,, \quad \text{and} \quad y(\xi,\eta,t) = \eta + \alpha(t)\sin(2\pi\xi)\sin(2\pi\eta)\,,$$

respectively, where $\alpha(t) \le 0.1$ and t is real parameter between 0 and 1; see [20]. The grid shown in Fig. 6.1 corresponds to $t = 0.5$ and $\alpha(t) = t/5$.

TABLE 6.1
Error data and estimated orders of convergence for the standard mixed Galerkin method (MG) and its mimetic reformulation (RMG) on trapezoidal grids.

error	method	33×33	65×65	129×129	order
$\|p - p^h\|_0$	MG	0.179E-01	0.893E-02	0.447E-02	0.9999
	RMG	0.179E-02	0.893E-02	0.447E-02	0.9999
$\|\mathbf{u} - \mathbf{u}^h\|_0$	MG	0.652E-01	0.325E-01	0.162E-01	1.0029
	RMG	0.652E-01	0.325E-01	0.162E-01	1.0029
$\|\nabla \cdot \mathbf{u} - \nabla \cdot \mathbf{u}^h\|_0$	MG	0.117E+01	0.110E+01	0.109E+01	0.0211
	RMG	0.117E+01	0.110E+01	0.109E+01	0.0211
$\|\nabla \cdot \mathbf{u} - \mathsf{DIV}(\mathbf{u}^h)\|_0$	MG	0.440E+00	0.220E+00	0.110E+00	1.0000
	RMG	0.440E+00	0.220E+00	0.110E+00	1.0000

TABLE 6.2
Error data and estimated orders of convergence for the standard mixed Galerkin method (MG) and its mimetic reformulation (RMG) on randomly perturbed grids.

error	method	33×33	65×65	129×129	order
$\|p - p^h\|_0$	MG	0.170E-01	0.848E-02	0.424E-02	1.000
	RMG	0.170E-01	0.848E-02	0.424E-02	1.000
$\|\mathbf{u} - \mathbf{u}^h\|_0$	MG	0.611E-01	0.308E-01	0.155E-01	1.000
	RMG	0.611E-01	0.308E-01	0.155E-01	1.000
$\|\nabla \cdot \mathbf{u} - \nabla \cdot \mathbf{u}^h\|_0$	MG	0.975E+00	0.890E+00	0.875E+00	0.025
	RMG	0.975E+00	0.890E+00	0.875E+00	0.025
$\|\nabla \cdot \mathbf{u} - \mathsf{DIV}(\mathbf{u}^h)\|_0$	MG	0.464E+00	0.232E+00	0.116E+00	1.000
	RMG	0.464E+00	0.232E+00	0.116E+00	1.000

TABLE 6.3
Error data and estimated orders of convergence for the standard mixed Galerkin method on sinusoidal grids.

error	33×33	65×65	129×129	order
$\|p - p^h\|_0$	0.184E-01	0.902E-02	0.449E-02	1.007
$\|\mathbf{u} - \mathbf{u}^h\|_0$	0.638E-01	0.318E-01	0.159E-01	1.001
$\|\nabla \cdot \mathbf{u} - \nabla \cdot \mathbf{u}^h\|_0$	0.576E+00	0.288E+00	0.144E+00	0.999
$\|\nabla \cdot \mathbf{u} - \mathsf{DIV}(\mathbf{u}^h)\|_0$	0.541E+00	0.271E+00	0.135E+00	0.999

order to make the tests more "realistic" and is not necessary at all to elicit the loss of convergence in the two standard methods. The latter can be observed even in the trivial case of $\Theta_1 = \mathbf{I}$ where $\mathbf{I}$ is a 2×2 unit matrix; see [4].

The mixed method and its reformulation. The presence of the reaction term in (1.1) or lack thereof do not affect the overall behavior of the computed error. For brevity, results without this term ($\sigma = 0$) are omitted. Error data and estimated

TABLE 6.4
Error data and estimated orders of convergence for the standard least-squares method (LS) and its mimetic reformulation (RLS) on trapezoidal grids: problem (1.1) with reaction term ($\sigma = 1$).

error	method	33×33	65×65	129×129	order
$\|p - p^h\|_0$	LS	0.863E-04	0.216E-04	0.541E-05	1.998
	RLS	0.876E-04	0.219E-04	0.549E-05	1.998
$\|\nabla(p - p^h)\|_0$	LS	0.1592E-01	0.799E-02	0.401E-02	0.997
	RLS	0.1592E-01	0.799E-02	0.401E-02	0.997
$\|\mathbf{u} - \mathbf{u}^h\|_0$	LS	0.675E-01	0.362E-01	0.225E-01	0.683
	RLS	0.652E-01	0.325E-01	0.162E-01	1.003
$\|\nabla \cdot \mathbf{u} - \nabla \cdot \mathbf{u}^h\|_0$	LS	0.115E+01	0.109E+01	0.107E+01	0.021
	RLS	–	–	–	–
$\|\nabla \cdot \mathbf{u} - \mathsf{DIV}(\mathbf{u}^h)\|_0$	LS	0.479E+00	0.285E+00	0.210E+00	0.439
	RLS	0.440E+00	0.220E+00	0.110E+00	1.000

convergence rates for (4.1) and its mimetic reformulation (4.6) on trapezoidal and randomly perturbed grids are summarized in Tables 6.1–6.2. The tables show identical[11] errors for both versions of the mixed method, which confirms the assertion of Theorem 5.1 that their solutions coincide.

As predicted by Theorem 5.1, when the divergence error of the velocity approximation is measured *directly* by DIV instead of *indirectly* by $\nabla\cdot$, the order of convergence improves to 1. This validates our assertion that the loss of convergence in the mixed method is superficial rather than real. It follows that a standard implementation of this method with the lowest-order Raviart-Thomas element is safe to use on general quadrilateral grids, as long as one remembers to extract the divergence information using DIV.

Table 6.3 shows error data and estimated convergence rates for the standard mixed method on the sinusoidal grid. Owing to the fact that this grid is nearly affine, the rates of convergence measured by using the analytic and the mimetic divergence operators are identical despite the small variations in their values.

The least-squares method and its reformulation. Theorem 4.1 suggests that the reaction term could be very important for the standard least-squares method. This turns out to be the case. Tables 6.4–6.5 show error data for (4.3) and (4.7) with this term ($\sigma = 1$) on trapezoidal and randomly perturbed grids, respectively. For the velocity in the standard method on both grids we see a reduced order of convergence in the L^2-norm and an almost complete loss of convergence in the divergence error. It is worth pointing out that using DIV to extract the divergence information from the standard least-squares solution does not help much. Nevertheless, the order of convergence in the divergence error is somewhat improved.

As predicted by Theorem 4.1, when the reaction term is present the loss of accuracy does not spread to the pressure approximation in the standard method. Tables 6.4–6.5 show the expected second and first-order convergence for the L^2 and H^1-seminorm errors of this variable, respectively.

[11] To avoid data variations caused by the randomness of the grid, for each grid size the two methods were run on the same instance of the random mesh.

TABLE 6.5
Error data and estimated orders of convergence for the standard least-squares method (LS) and its mimetic reformulation (RLS) on randomly perturbed grids: problem (1.1) with reaction term ($\sigma = 1$).

error	method	33×33	65×65	129×129	order
$\|p - p^h\|_0$	LS	0.650E-04	0.167E-04	0.414E-05	2.008
	RLS	0.733E-04	0.200E-04	0.505E-05	1.984
$\|\nabla(p - p^h)\|_0$	LS	0.146E-01	0.734E-02	0.366E-02	1.003
	RLS	0.148E-01	0.742E-02	0.372E-02	0.996
$\|\mathbf{u} - \mathbf{u}^h\|_0$	LS	0.627E-01	0.326E-01	0.185E-01	0.815
	RLS	0.611E-01	0.308E-01	0.154E-01	0.999
$\|\nabla \cdot \mathbf{u} - \nabla \cdot \mathbf{u}^h\|_0$	LS	0.942E+00	0.882E+00	0.858E+00	0.040
	RLS	–	–	–	–
$\|\nabla \cdot \mathbf{u} - \mathsf{DIV}(\mathbf{u}^h)\|_0$	LS	0.484E+00	0.271E+00	0.190E+00	0.511
	RLS	0.463E+00	0.232E+00	0.116E+00	1.001

TABLE 6.6
Error data and estimated orders of convergence for the standard least-squares method (LS) and its mimetic reformulation (RLS) on trapezoidal grids: problem (1.1) without reaction term ($\sigma = 0$).

error	method	33×33	65×65	129×129	order
$\|p - p^h\|_0$	LS	0.175E-02	0.150E-02	0.144E-02	0.060
	RLS	0.378E-03	0.947E-04	0.237E-04	1.999
$\|\nabla(p - p^h)\|_0$	LS	0.201E-01	0.136E-01	0.114E-01	0.254
	RLS	0.161E-01	0.801E-02	0.401E-02	0.999
$\|\mathbf{u} - \mathbf{u}^h\|_0$	LS	0.676E-01	0.363E-01	0.227E-01	0.678
	RLS	0.652E-01	0.325E-01	0.162E-01	1.003
$\|\nabla \cdot \mathbf{u} - \nabla \cdot \mathbf{u}^h\|_0$	LS	0.115E+01	0.109E+01	0.107E+01	0.021
	RLS	–	–	–	–
$\|\nabla \cdot \mathbf{u} - \mathsf{DIV}(\mathbf{u}^h)\|_0$	LS	0.479E+00	0.285E+00	0.211E+00	0.437
	RLS	0.440E+00	0.220E+00	0.110E+00	1.000

In the absence of the reaction term, the standard least-squares method fares much worse. Tables 6.6–6.7 show that the loss of accuracy on trapezoidal and randomly perturbed grids when $\sigma = 0$ affects both variables. We see that without the reaction term, the L^2 order of convergence of the pressure is completely ruined, and the H^1-seminorm error is severely reduced. These results are consistent with the numerical data on trapezoidal grids presented in [4] and confirm that, unlike in the mixed method, the loss of accuracy in the least-squares method is real. Inclusion of the reaction term helps to stem the deterioration of the pressure approximation but, as a whole, the standard version of the least-squares method cannot be deemed robust enough for general quadrilateral grids.

As expected, the mimetic reformulation of the least-squares method completely eliminates these problems. From the data in Tables 6.4–6.7 we see that the reformu-

TABLE 6.7
Error data and estimated orders of convergence for the standard least-squares method (LS) and its mimetic reformulation (RLS) on random grids: problem (1.1) without reaction term ($\sigma = 0$).

error	method	33×33	65×65	129×129	order
$\|p - p^h\|_0$	LS	0.123E-02	0.101E-02	0.951E-03	0.082
	RLS	0.396E-03	0.973E-04	0.251E-04	1.956
$\|\nabla(p - p^h)\|_0$	LS	0.169E-01	0.104E-01	0.793E-02	0.388
	RLS	0.152E-01	0.745E-02	0.373E-02	0.997
$\|\mathbf{u} - \mathbf{u}^h\|_0$	LS	0.624E-01	0.328E-01	0.186E-01	0.816
	RLS	0.610E-01	0.308E-01	0.153E-01	1.005
$\|\nabla \cdot \mathbf{u} - \nabla \cdot \mathbf{u}^h\|_0$	LS	0.930E+00	0.874E+00	0.861E+00	0.021
	RLS	–	–	–	–
$\|\nabla \cdot \mathbf{u} - \mathsf{DIV}(\mathbf{u}^h)\|_0$	LS	0.489E+00	0.273E+00	0.186E+00	0.553
	RLS	0.463E+00	0.233E+00	0.116E+00	1.003

TABLE 6.8
Error data and estimated orders of convergence for the standard least-squares method (LS) on sinusoidal grids: problem (1.1) with (sigma = 1) and without (sigma = 0) reaction term.

error	method	33×33	65×65	129×129	order
$\|p - p^h\|_0$	$\sigma = 0$	0.598E-03	0.151E-03	0.379E-04	1.996
	$\sigma = 1$	0.158E-03	0.400E-04	0.100E-04	1.996
$\|\nabla(p - p^h)\|_0$	$\sigma = 0$	0.184E-01	0.902E-02	0.449E-02	1.007
	$\sigma = 1$	0.179E-01	0.896E-02	0.448E-02	1.000
$\|\mathbf{u} - \mathbf{u}^h\|_0$	$\sigma = 0$	0.638E-01	0.318E-01	0.159E-01	1.001
	$\sigma = 1$	0.638E-01	0.318E-01	0.159E-01	1.001
$\|\nabla \cdot \mathbf{u} - \nabla \cdot \mathbf{u}^h\|_0$	$\sigma = 0$	0.576E+00	0.288E+00	0.144E+00	1.000
	$\sigma = 1$	0.576E+00	0.288E+00	0.144E+00	1.000
$\|\nabla \cdot \mathbf{u} - \mathsf{DIV}(\mathbf{u}^h)\|_0$	$\sigma = 0$	0.541E+00	0.271E+00	0.135E+00	1.000
	$\sigma = 1$	0.541E+00	0.271E+00	0.135E+00	1.000

lation restores the optimal order of convergence for all variables regardless of whether or not the reaction terms is included.

Finally, Table 6.8 shows error and convergence data for the standard least-squares method on sinusoidal grids. We see that despite the highly distorted nature of this grid, the fact that most of its elements remain close to affine quads is enough to restore convergence rates for all variables.

7. Conclusions. The mimetic reformulation, proposed in this paper, is a simple yet effective approach to restore convergence of finite element methods that employ the lowest-order quadrilateral Raviart-Thomas elements.

By proving that the reformulation of the mixed method is equivalent to its standard version, we establish that the loss of convergence in this method is benign and can be avoided by using DIV to compute the divergence of the velocity approximation.

Our results also show that the deterioration of accuracy in the least-squares method is real. For problems with a reaction term it is confined to the velocity approximation, but without this term, the loss of convergence spreads to both variables. The mimetic reformulation of the least-squares method mitigates convergence problems and should be used whenever computations with this method involve non-affine quadrilateral grids.

Acknowledgments. We thank the anonymous referees for several suggestions that helped to improve the paper and prompted us to include more informative numerical examples and data.

REFERENCES

[1] T. Arbogast, C. Dawson, P. Keenan, M. Wheeler, I. Yotov, *Enhanced cell-centered finite differences for elliptic equations on general geometry*, SIAM J. Sci. Comp., 19/2, pp. 404-425, 1998.

[2] V. Arnold Mathematical Methods of Classical Mechanics, Springer, 1989.

[3] D. N. Arnold, D. Boffi, and R. S. Falk, *Approximation by quadrilateral finite elements*, Math. Comp., 71 (2002), pp. 909-922.

[4] D.N. Arnold, D. Boffi, and R.S. Falk, *Quadrilateral $H(div)$ finite elements.* SIAM J. Numer. Anal. 42, pp. 2429-2451, 2005.

[5] M. Berndt, K. Lipnikov, M. Shashkov, M.F. Wheeler and I. Yotov, *Superconvergence of the Velocity in Mimetic Finite Difference Methods on Quadrilaterals*, SIAM J. Numer. Anal., Vol. 43, No. 4, pp. 1728–1749, 2005.

[6] P. Bochev and M. Gunzburger, *Finite element methods of least-squares type*, SIAM Review , Vol. 40, Issue 4 pp. 789–837, 1998 .

[7] P. Bochev and M. Gunzburger, *On least-squares finite elements for the Poisson equation and their connection to the Kelvin and Dirichlet principles*, SIAM J. Num. Anal. 43/1. pp. 340-362, 2005.

[8] P. Bochev and M. Gunzburger, *A locally conservative least-squares method for Darcy flows*, Communications in Numerical Methods in Engineering, Published online December 1, 2006, DOI10.1002/cnm.957,

[9] D. Boffi, F. Kikuchi, and J. Schberl. *Edge element computation of Maxwell's eigenvalues on general quadrilateral meshes.* Mathematical Models and Methods in Applied Sciences, 16(2), 2006, pp. 265-273.

[10] D. Boffi and L. Gastaldi. *Some remarks on quadrilateral mixed finite elements.* Submitted to the fifth MIT conference.

[11] F. Brezzi, *On existence, uniqueness and approximation of saddle-point problems arising from Lagrange multipliers*, RAIRO Model. Math. Anal. Numer., 21, pp. 129–151, 1974.

[12] F. Brezzi and M. Fortin, *Mixed and Hybrid Finite Element Methods*, Springer, Berlin, 1991.

[13] P. Ciarlet, *The finite element method for elliptic problems*, SIAM, SIAM Classics in Applied Mathematics, 2002.

[14] G. Fix, M. Gunzburger and R. Nicolaides; On finite element methods of the least-squares type; *Comput. Math. Appl.* 5, pp. 87-98, 1979.

[15] V. Girault and P. Raviart, *Finite Element Methods for Navier-Stokes Equations*, Springer, Berlin, 1986.

[16] J. Hyman, and M. Shashkov; *Natural discretizations for the divergence, gradient and curl on logically rectangular grids*; Comput. Math. Appl. 33, pp. 88-104, 1997.

[17] J. Hyman and M. Shashkov, *Adjoint operators for the natural discretizations of the divergence, gradient and curl on logically rectangular grids*, Appl. Num. Math., 25, pp.413–442, 1997.

[18] J. Hyman and M. Shashkov, *The orthogonal decomposition theorems for mimetic finite difference schemes*, SIAM J. Num. Anal., 36, pp.788–818, 1999.

[19] Y. Kuznetsov and S. Repin. *Convergence analysis and error estimates for mixed finite element method on distorted meshes.* J. Numer. Math., 13(1):3351, 2005.

[20] L.G. Margolin, and M. Shashkov, *Second-order sign-preserving conservative interpolation (remapping) on general grids*, J. Comp. Phys. 184, (2003) pp. 266-298.

[21] P.A. Raviart and J.M. Thomas, *A mixed finite element method for second order elliptic problems*, Mathematical aspects of the finite element method, I, Galligani and E. Magenes, Lecture Notes in Math., 606, Springer-Verlag, New York, 1977.

[22] M. Shashkov, *Conservative finite difference methods on general grids*, CRC Press, Boca Raton, FL, 1996.

[23] J. Shen. *Mixed finite element methods on distorted rectangular grids.* Technical Report ISC-94-13-MATH, Texas A&M University, 1994.

[24] M. Wheeler and I. Yotov, *A cell-centered finite difference method on quadrilaterals.* In *Compatible spatial discretizations*, D. Arnold, P. Bochev, R. Lehoucq, R. Nicolaides, M. Shashkov, eds., The IMA volumes in mathematics and its Applications, Vol. 142, pp.189–207, 2006.